

Doping evolution of chemical potential, spin-correlation gap, and charge dynamics in $\text{Nd}_{2-x}\text{Ce}_x\text{CuO}_4$

N. L. Wang,¹ G. Li,¹ D. Wu,¹ X. H. Chen,² C. H. Wang,² and H. Ding³

¹*Beijing National Laboratory for Condensed Matter Physics, Institute of Physics, Chinese Academy of Sciences, Beijing 100080, P. R. China*

²*Hefei National Laboratory for Physics Science at Microscale and Department of Physics, University of Science and Technology of China, Hefei 230026, P. R. China*

³*Department of Physics, Boston College, Chestnut Hill, MA 02467, USA*

We report optical reflectivity study on $\text{Nd}_{2-x}\text{Ce}_x\text{CuO}_4$ over a broad doping range $0 \leq x \leq 0.20$. The study reveals a systematic shift of chemical potential with doping. A pronounced peak structure specific to the electron-doped cuprate is observed in optical scattering rate based on the extended Drude model analysis. The energy scale of the peak could be very different from that of the peak in conductivity spectrum. We clarify that the "hot spots" gap probed in photoemission experiments correlates directly with the sharp suppression feature in scattering rate rather than conductivity spectra. The gap is associated with the short-range antiferromagnetic correlation, and disappears in a manner of fading away with increasing doping and temperature. In the heavily overdoped region, a dominant ω^2 -dependence of the scattering rate is identified up to very high energy.

PACS numbers: 74.25.Gz, 74.72.Jt, 74.25.Dw, 74.25.Jb

I. INTRODUCTION

A central issue in understanding the mechanism of high-temperature superconductivity is how an antiferromagnetic (AF) insulator evolves into a superconductor with electron or hole doping. Although both the electron- and hole-doped high- T_c superconductors share a lot of similarities, including the d-wave pairing symmetry, the phase diagrams exhibit rather asymmetric behaviors¹. For the hole-doped cuprates, the AF order disappears with a small amount of carrier concentration, and the superconducting phase is well separated from the AF ordered phase; while in the electron-doped cuprates, the AF order is much more robust with respect to doping, and the AF and superconducting phases are adjacent to each other or even coexist. The doping range where the superconducting transition occurs in electron-doped cuprates is much narrower and the maximum T_c is much lower than for hole doped cuprates. Angle-resolved photoelectron spectroscopy (ARPES) experiments indicated that the hole carriers doped into the parent compound first enter $(\pi/2, \pi/2)$ points in the Brillouin zone and produce a Fermi arc². By contrast, for the electron-doped case, a small Fermi surface pocket appears first around $(\pi, 0)$, and another one shows up around $(\pi/2, \pi/2)$ upon increasing doping. The two pockets are separated by a gaped region locating at the intersecting points (so-called "hot spots") of the Fermi surface and the AF zone boundary³.

Optical spectroscopy can probe not only the low-lying intraband response, but also the interband transitions from occupied to unoccupied states. It provides supplementary information about the electronic states as yielded by ARPES, which detects only occupied states. Previous optical studies on $\text{Nd}_{2-x}\text{Ce}_x\text{CuO}_4$ (NCCO) system^{4,5,6,7} have uncovered a transfer of spectral weight from charge-transfer excitations to low frequencies with

doping, and an occurrence of a large pseudogap in optical conductivity, which is believed to be a reflection of the gaped region in the Fermi surface seen in ARPES experiment. A recent doping-dependent optical study further suggested that this partial gap is associated with an ordered phase which ends on a quantum critical point at approximately optimal doping⁸. In this paper, we present a more systematic optical study on NCCO single crystals. Our samples cover very broad doping range from parent compound to overdoped non-superconducting compound. The study reveals a number of novel properties, including a systematic shift of chemical potential, a spin-correlation gap which fades away with doping/temperature with no clear phase boundary line, and a dominant ω^2 -dependence of the scattering rate up to very high energy in the non-superconducting overdoped region. We clarify that the "hot spots" gap probed in ARPES experiments correlates directly with the gap in the scattering rate spectrum rather than with the suppression feature in optical conductivity spectrum.

II. EXPERIMENTS

The NCCO single crystals were grown from a copper-oxide-rich melt in Al_2O_3 crucibles over a wide range of Ce concentration $0 \leq x \leq 0.20$. The actual Ce concentration was determined by inductively coupled plasma spectrometry analysis experiments, and by the energy-dispersive x-ray analysis using a scanning electron microscopy, respectively. All samples were annealed in flowing helium for over 10 hours at 900°C to remove the interstitial oxygen.

The near-normal incident reflectance spectra ($R(\omega)$) were measured by a Bruker 66v/s spectrometer in the frequency range from 50 cm^{-1} to $25,000 \text{ cm}^{-1}$. The crystal with a very shiny surface was mounted on an opti-

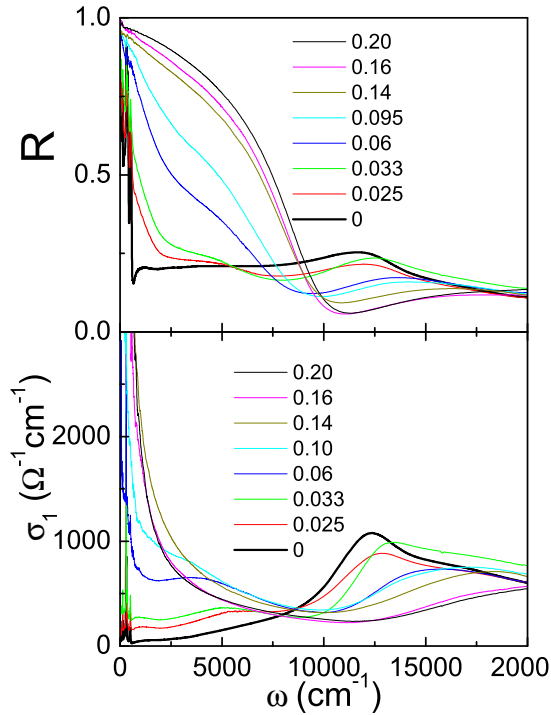


FIG. 1: (Color online) The evolution of in-plane reflectance and conductivity spectra for $\text{Nd}_{2-x}\text{Ce}_x\text{CuO}_4$ with dop

cally black cone in a cold-finger flow cryostat. An *in situ* gold and aluminum overcoating technique was employed for reflectance measurements⁹. The optical conductivity spectra were obtained from a Kramers-Kronig transformation of $R(\omega)$. We use Hagen-Rubens relation for the low frequency extrapolation, and a constant extrapolation to $100,000 \text{ cm}^{-1}$ followed by a well-known function of ω^{-4} in the higher-energy side.

III. CHEMICAL POTENTIAL SHIFT WITH DOPING

Figures. 1 shows the room temperature $R(\omega)$ and conductivity ($\sigma_1(\omega)$) spectra for NCCO. The undoped $x=0$ crystal shows a broad peak at 1.5 eV (12000 cm^{-1}) due to the charge-transfer excitations. At low frequency, it has very low conductivity values except for some infrared-active phonon lines. Upon Ce substitution, a transfer of spectral weight from charge-transfer excitations to low frequency occurs. A mid-infrared broad peak at about $4000\text{-}5000 \text{ cm}^{-1}$ is formed first at low doping, then a Drude component appears at lower frequencies with further doping. Such spectral change has been observed previously^{4,5,7} and shares many similarities with the hole-doped cuprates¹⁰. However, one important feature which was not addressed previously is that, accompanying the spectral weight transfer, the charge-transfer excitation peak also shifts gradually to higher frequencies with in-

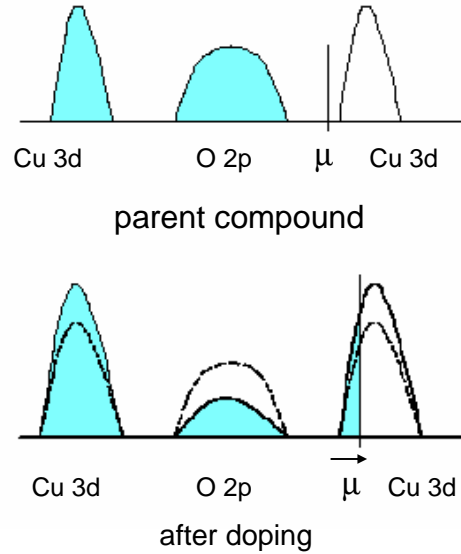


FIG. 2: (Color online) A schematic picture for the doping evolution of electronic states of $\text{Nd}_{2-x}\text{Ce}_x\text{CuO}_4$. For undoped parent compound, the chemical potential locates close to the Cu 3d upper Hubbard band. With electron doping, the chemical potential moves into the conduction band and shifts up.

creasing doping. This behavior is associated with the change of chemical potential with electron doping, as elaborated below.

It is useful to compare the above result with ARPES data. ARPES measurement on undoped Nd_2CuO_4 revealed a dispersion band $\sim 1.3 \text{ eV}$ below the chemical potential μ along zone diagonal, which was ascribed to the oxygen-derived charge transfer band³. Note that this energy (1.3 eV) is lower than the charge-transfer excitation ($\sim 1.5 \text{ eV}$) seen in optical measurement. As we mentioned, the ARPES experiment detects the occupied states relative to the chemical potential, while optics probes the interband transition from an occupied band below μ to an unoccupied band above μ . The small difference between the two probes indicates that the μ locates just slightly below the Cu 3d upper Hubbard band in Nd_2CuO_4 (Fig.2). By contrast, the μ for the hope-type parent compound La_2CuO_4 is close to the oxygen 2p band. This is because the dispersive band seen in ARPES measurement is not far from the Fermi level², while the charge-transfer excitations probed by optical measurement are around 2 eV ¹⁰. The fact that μ is very close to the Cu 3d upper Hubbard band in Nd_2CuO_4 and to the O 2p band in La_2CuO_4 explains why electrons and hole are easily doped into those different types of compounds, respectively.

There exists a long standing controversy over the evolution of μ with doping in cuprates¹. One simple picture is that μ moves into the valence or conduction band as the material is doped away from half filling with holes or electrons, respectively. Another opinion is that car-

rier doping creates "states" inside the insulator's gap, but μ remains relatively fixed in the middle of the gap. It is difficult to get to a definite solution to this issue solely from APRES measurement. In fact, the experimental data on different materials have been interpreted in terms of both scenarios^{11,12,13}. The present optical experiments, showing a shift of charge-transfer excitation with doping, is obviously consistent with the scenario that the μ enters the upper Cu 3d Hubbard band and shifts up with electron doping. As illustrated in Fig. 2, when the chemical potential moves into the valence band, some states in Cu 3d upper Hubbard band were occupied, then the charge-transfer transition from the oxygen 2p to upper Cu 3d Hubbard band would require a bit higher energy than the charge-transfer gap. The chemical potential shift in NCCO was also seen in a core-level photoemission study¹⁴.

IV. EVOLUTION OF "HOT SPOTS" GAP

A. Gap features in conductivity and scattering rate spectra

Figure 3 shows the T -dependent $R(\omega)$ spectra for several doping levels $x=0.06, 0.10, 0.14,$ and 0.20 , respectively. The $x=0.06$ and $x=0.10$ samples are heavily underdoped and locate below the superconducting region, the $x=0.14$ sample is slightly underdoped with $T_c \approx 18$ K, while the $x=0.20$ sample is highly overdoped and also out of the superconducting region in the phase diagram. The most prominent feature is a reverse S-shape at low T for the underdoped samples. Correspondingly, the conductivity spectra, displayed in the upper panels of Fig. 4, show suppressions of spectral weight below ~ 0.5 eV (4000 cm^{-1}). Such behavior was observed in previous optical measurement and referred to as a pseudogap⁷. The suppressions are clearly seen for $x=0.06$ and 0.10 samples, and are also present in the low- T curves for the $x=0.14$ superconductor. In the mean time, Drude-like peaks are still seen at very low frequency for all those samples, evidencing metallic responses in both T - and ω -dependences. Those observations indicate clearly that the gap appears only on parts of the Fermi surface. The Drude-type contribution originates from the gapless regions of the Fermi surface.

The dynamics of charge carriers is usually described in terms of frequency-dependent scattering rate on the basis of the extended Drude model,

$$\frac{1}{\tau(\omega)} = \frac{\omega_p^2}{4\pi} \text{Re} \frac{1}{\sigma(\omega)}, \quad (1)$$

where $\sigma(\omega) = \sigma_1(\omega) + i\sigma_2(\omega)$ is the complex conductivity, ω_p is the plasma frequency which can be obtained by summarizing $\sigma_1(\omega)$ up to the reflectance edge frequency. The scattering rate spectra for the above four samples are shown in the bottom panels of Fig. 4. Related to

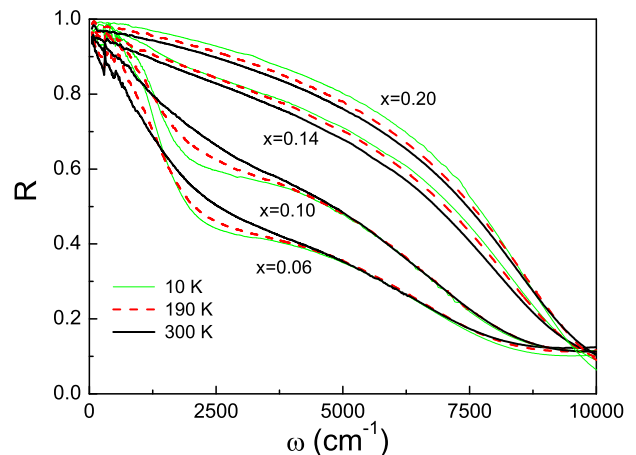


FIG. 3: (Color online) The temperature dependence of the reflectance spectra for several doping levels.

the suppression in $\sigma_1(\omega)$ spectrum, we observe a peak in $1/\tau(\omega)$ for underdoped $\text{Nd}_{2-x}\text{Ce}_x\text{CuO}_4$ samples, below which the scattering rate is strongly suppressed.

It should be noted that a depression of $1/\tau(\omega)$ at low frequencies followed by a peak or overshoot at high frequencies is also a characteristic feature for a gaped state. To explain such structure, Basov et al.¹⁵ introduced an approximate sum rule for the difference between energy-dependent scattering rates:

$$\int_0^{\omega_c} d\omega \left(\frac{1}{\tau^A(\omega)} - \frac{1}{\tau^B(\omega)} \right) \simeq 0. \quad (2)$$

where indexes A and B refer to different states of the studied system (e.g., normal, pseudogap, superconducting). This sum rule is based on the exact value of the imaginary part of the loss function,

$$\int_0^{\infty} \frac{d\omega}{\omega} \text{Im}[\epsilon^{-1}(\omega, T)] = -\frac{\pi}{2}. \quad (3)$$

In the case of $\omega < \omega_p$, the scattering rate can be expressed as $1/\tau(\omega) \approx \omega_p^{-1} \text{Im}(1/\epsilon)$ and therefore the sum rule is obeyed. According to equation (2), the suppression of $1/\tau(\omega)$ in the intragap region ought to be balanced out by the overshoot at $\omega > E_g$.¹⁵ Indeed, such characteristic structure, *i.e.* a decrease and then an overshoot in $1/\tau(\omega)$, was found to be present in materials with development of different sorts of gaps. For example, the behaviors were seen in antiferromagnet Cr where a spin-density-wave (SDW) gap opens on parts of the Fermi surface¹⁵, and in the heavy-fermion materials $\text{YbFe}_4\text{Sb}_{12}$ and UPd_2Al_3 where hybridization gaps due to the mixing of the f band and the conduction band open on parts of the Fermi surface^{15,16}.

In high- T_c cuprates, the effect of the formation of a superconducting gap or the development of a pseudogap on the scattering rate is more complicated. Due to the fact that the in-plane carrier dynamics is governed by the nodal region of the Fermi surface that remains gapless at all temperature, the gap effect is usually

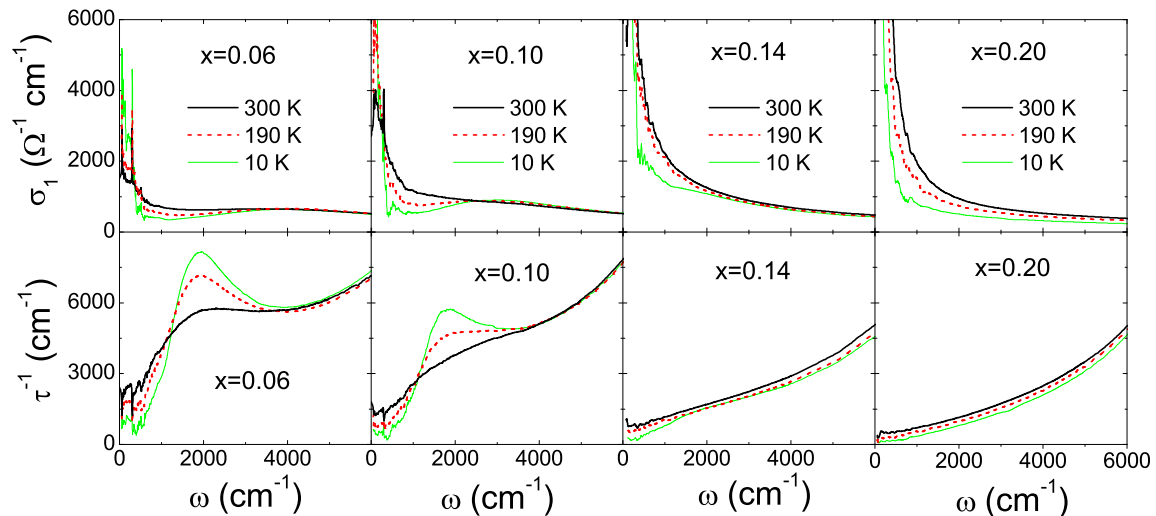


FIG. 4: (Color online) The temperature dependence of the conductivity and scattering rate spectra for $x=0.06, 0.10, 0.14$ and 0.20 samples.

very weak. For optimally doped YBCO¹⁵ and Tl-based systems¹⁷, a small overshoot shows up immediately above the suppression in $1/\tau(\omega)$ in the superconducting state. However, for underdoped cuprates, particularly in the pseudogap state, the overshoot is usually not observed, the spectral weight lost at low ω is not recovered up to the highest frequency measured. A thorough discussion about the respective effects of superconducting gaps with s-wave and d-wave symmetries on the sum rules for $1/\tau(\omega)$ was provided by Marsiglio *et al.*¹⁸. Nevertheless, for the electron-doped compounds under present investigation, the $1/\tau(\omega)$ spectra display significant peak structures just above the suppressions. The energy scale of the peak is much larger than that of the small overshoot below T_c in $1/\tau(\omega)$ for hole-type cuprates at optimal doping. Therefore, the structure is specific to electron-doped cuprates. It provides strong evidence for the gap formation on the Fermi surface in the underdoped NCCO. Apparently, the gaps in the present case are not superconducting ones, but correspond to gaps at "hot spots" with a much larger energy scale. Because the hot spots locate more closely to the nodal region, the gap features are seen more pronounced.

B. Different energy scales for the peaks in $\sigma_1(\omega)$ and $1/\tau(\omega)$ and their evolutions with doping

We notice that the peak positions in $1/\tau(\omega)$ spectra can be quite different from the peak positions in $\sigma_1(\omega)$ spectra. For example, in the $x=0.06$ sample, the peak in $\sigma_1(\omega)$ locates near 4000 cm^{-1} , while the peak in $1/\tau(\omega)$ is only around 2000 cm^{-1} . A natural question is which one reflects the gap amplitude? Previously, the pseudogap observed in optics and its connection with the gap seen in ARPES was established from $\sigma_1(\omega)$ spectra⁷, but this

should be reexamined.

It is worth mentioning that there is no simple and direct connection between the quantity $\sigma_1(\omega)$ or $1/\tau(\omega)$ and the density of states (DOS). In order to know the gap magnitude, one needs a model to derive those optical quantities which, in general, involve a summation over the full Fermi surface. As there is no theoretical study available for distinguishing the gap features in the two optical quantities, we consider a special case here. We calculate the conductivity spectra for a standard BCS model with an energy gap of 2Δ in both clean and dirty limits for $T \ll T_c$,¹⁹ then determine $1/\tau(\omega)$ from the extended Drude model (equ. (1)). The model is applicable to both the superconducting and the CDW/SDW gaps. The results are shown in Fig. 5. The calculation well reproduces the sharp peak structure near 2Δ in $1/\tau(\omega)$ as obtained by Basov *et al.*¹⁵, which is due to the presence of a singularity of DOS. It indicates clearly that, for the same strength of impurity scattering, the peak position in $\sigma_1(\omega)$ could be very different from that in $1/\tau(\omega)$, although both can occur above the gap energy. The peak in $\sigma_1(\omega)$ always appears at a higher energy. But the energy difference between the peaks in $\sigma_1(\omega)$ and $1/\tau(\omega)$ becomes smaller with reducing the impurity scattering due to a faster shift of the peak position towards the low frequency in $\sigma_1(\omega)$. On this account, the gap energy is much closer to the peak energy in $1/\tau(\omega)$ than that in $\sigma_1(\omega)$.

Although the calculations are for the case of a fully gapped Fermi surface, the experimental data for the "hot spot" gaps of NCCO (i.e. partial gaps in the Fermi surface) qualitatively follow the trend both in the peak positions and with doping evolution. Since the electrons in heavily underdoped samples experience stronger scattering, a larger energy difference between those peaks was observed, as one would expect. Additionally, the gap

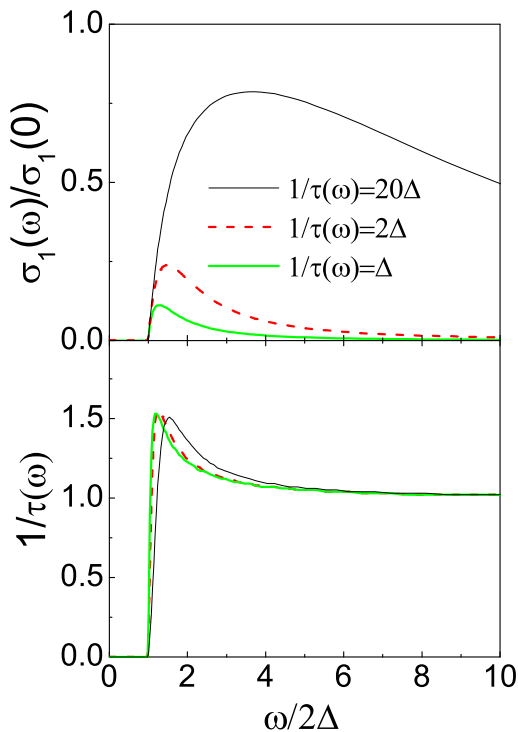


FIG. 5: (Color online) The calculated conductivity and scattering rate spectra for a BCS model ($T \ll T_c$) in both the clean and dirty limits with $(1/\tau)/\Delta=1, 2,$ and 20 .

magnitude in $1/\tau(\omega)$ is indeed comparable to the gap energy seen in ARPES measurement. ARPES experiments have well established that the partial energy gap locates at the intersecting points (hot spots) of the Fermi surface with the AF zone boundary, pointing towards a SDW-type origin due to the strong AF scattering. Matsui *et al.* recently measured the T -dependent ARPES spectra on a NCCO crystal at $x=0.13$,²⁰ and identified a maximum gap (i.e. a hump feature in an energy dispersion curve) ~ 0.19 eV. This value is very close to the peak positions in $1/\tau(\omega)$ for the compounds with similar Ce contents.

We now address the evolution of the AF gap with doping. From Fig. 4, we found that the peak in $1/\tau(\omega)$ shows much less frequency shift than the suppression feature in $\sigma_1(\omega)$ with increasing doping. The most prominent change is a weakening of the gap structure with increasing doping and temperature. The results suggest that the disappearance of the gap feature is not due to the reduction of the gap energy, but in a manner of gradually fading away. The result is well consistent with Raman scattering data on the two-magnon peak: its intensity decreases with Ce doping but the peak energy shows little doping dependence⁷. ARPES data on the underdoped $\text{Nd}_{1.87}\text{Ce}_{0.13}\text{CuO}_4$ further indicated that the AF pseudogap was gradually filling up with increasing T without showing any observable shift in energy²⁰. Note that although the gap is due to the AF scattering²¹, it opens

at a temperature much higher than the AF ordered Neel temperature T_N or in a doping region where there is no long range AF ordering. Clearly, the gap already shows up when the short range AF correlation exists. Unlike the AF long range order which has a definite phase transition temperature, the AF short range order is a gradually evolving behavior with no phase line as a function of doping. Some authors suggest the existence of a quantum phase transition in the phase diagram for electron-doped cuprates^{8,22}. However, our analysis above suggested that the gap feature is associated with the short range AF interaction, with no clear boundary line or any critical point.

Another important feature is that, when the pseudogap goes away by further increasing doping, the $1/\tau(\omega)$ indicates a dominant ω^2 -dependence (see the $1/\tau(\omega)$ spectra for the $x=0.20$ samples in Fig. 4), suggesting a Fermi liquid-like state. The $1/\tau(\omega)$ spectra of the $x=0.14$ sample deviate from such ω^2 -dependence at the low frequency even at room temperature, suggesting that the short-range AF correlation is still effective at this doping level and temperature range. We believe that, at heavily overdoped region, due to the disappearance of the AF correlation, the magnetic folding of the Fermi surface vanishes completely, consequently only a single large Fermi surface centered at (π, π) is formed. The amazing observation is that this ω^2 -dependence goes up to the very high frequency, beyond 6000 cm^{-1} as shown in Fig. 4. This is very different from the hole doped cuprates. In the hole doped case, the scattering rate follows a linear ω -dependence which is well described by the Marginal Fermi liquid theory, whereas at high frequencies (around 0.5 eV) a saturation of $1/\tau(\omega)$ is commonly observed²³.

V. SUMMARY

Our systematic study on the NCCO crystals reveals a number of novel properties: (1) The chemical potential is not pinned in the gap region, but shifts up with electron doping. (2) Both ω -dependent conductivity and scattering rate spectra exhibit characteristic structures caused by "hot spots" gaps in the Fermi surface for underdoped samples. The peak position in $1/\tau(\omega)$ is found to be quite different from the peak position in $1/\sigma(\omega)$. We clarify that the "hot spots" gap probed by ARPES experiments correlates directly with the suppression feature in $1/\tau(\omega)$ rather than in optical conductivity spectra. (3) The gap becomes weaker with increasing doping/temperature and disappears in a manner of fading away. There is no clear phase transition line for the gap vanishing. (4) In the heavily overdoped region, the gap structure disappears completely due to the absence of the AF correlation, and a single large Fermi surface should be formed. We identify a ω^2 -dependence of $1/\tau(\omega)$ up to very high energy with no indication of saturation.

VI. ACKNOWLEDGEMENT

We acknowledge helpful discussions with D. N. Basov, J. L. Luo, T. Timusk, T. Tohyama, Z. Y. Weng, and T. Xiang. This work was supported by National Sci-

ence Foundation of China, the Knowledge Innovation Project of Chinese Academy of Sciences, and the Ministry of Science and Technology of China973 project No:2006CB601002). HD acknowledges the support from US NSF DMR-0353108.

-
- ¹ A. Damascelli, Z. Hussain and Z. X. Shen, *Rev. Mod. Phys.* **75**, 473 (2003).
- ² T. Yoshida, X. J. Zhou, T. Sasagawa, W. L. Yang, P. V. Bogdanov, A. Lanzara, Z. Hussain, T. Mizokawa, A. Fujimori, H. Eisaki, Z.-X. Shen, T. Kakeshita, and S. Uchida, *Phys. Rev. Lett.* **91**, 027001 (2003).
- ³ N. P. Armitage, D. H. Lu, C. Kim, A. Damascelli, K. M. Shen, F. Ronning, D. L. Feng, P. Bogdanov, Z.-X. Shen, Y. Onose, Y. Taguchi, Y. Tokura, P. K. Mang, N. Kaneko, and M. Greven, *Phys. Rev. Lett.* **87**, 147003 (2001); N. P. Armitage, F. Ronning, D. H. Lu, C. Kim, A. Damascelli, K. M. Shen, D. L. Feng, H. Eisaki, Z.-X. Shen, P. K. Mang, N. Kaneko, and M. Greven, Y. Onose, Y. Taguchi, and Y. Tokura, *ibid* **88**, 257001 (2002).
- ⁴ S. L. Cooper, G. A. Thomas, J. Orenstein, D. H. Rapkine, A. J. Millis, S. W. Cheong, A. S. Cooper, and Z. Fisk, *Phys. Rev. B* **41**, 11605 (1990).
- ⁵ T. Arima, Y. Tokura, and S. Uchida, *Phys. Rev. B* **48**, 6597 (1993).
- ⁶ E. J. Singley, D. N. Basov, K. Kurahashi, T. Uefuji, and K. Yamada, *Phys. Rev. B* **64**, 224503 (2001).
- ⁷ Y. Onose, Y. Taguchi, K. Ishizaka, and Y. Tokura, *Phys. Rev. Lett.* **87**, 217001 (2001); Y. Onose, Y. Taguchi, K. Ishizaka, and Y. Tokura *Phys. Rev. B* **69**, 024504 (2004).
- ⁸ A. Zimmers, J.M. Tomczak, R.P.S.M. Lobo, N. Bontemps, C.P. Hill, M.C. Barr, Y. Dagan, R.L. Greene, A.J. Millis, and C.C. Homes, *Europhys. Lett.* **70**, 225 (2005).
- ⁹ C. C. Homes, M. Reedyk, D.A. Crandles, and T. Timusk, *Appl. Opt.* **32**, 2976 (1993).
- ¹⁰ S. Uchida, T. Ido, H. Takagi, T. Arima, Y. Tokura, and S. Tajima, *Phys. Rev. B* **43**, 7942 (1991).
- ¹¹ J. W. Allen, C. G. Olson, M. B. Maple, J. S. Kang, L. Z. Liu, J. H. Park, R. O. Anderson, W. P. Ellis, J. T. Markert, Y. Dalichaouch, and R. Liu, *Phys. Rev. Lett.* **64**, 595 (1990).
- ¹² A. Ino, C. Kim, M. Nakamura, T. Yoshida, T. Mizokawa, Z.-X. Shen, A. Fujimori, T. Kakeshita, H. Eisaki, and S. Uchida, *Phys. Rev. B* **62**, 4137 (2000).
- ¹³ M. A. van Veenendaal, G. A. Sawatzky, and W. A. Groen, *Phys. Rev. B* **49**, 1407 (1994).
- ¹⁴ N. Harima, J. Matsuno, A. Fujimori, Y. Onose, Y. Taguchi, and Y. Tokura, *Phys. Rev. B* **64**, 220507(R) (2001).
- ¹⁵ D. N. Basov, E. J. Singley, and S. V. Dordevic, *Phys. Rev. B* **65**, 054516 (2002).
- ¹⁶ M. Dressel, N. Kasper, K. Petukhov, D. N. Peligrad, B. Gorshunov, M. Jourdan, M. Huth, and H. Adrian, *Phys. Rev. B* **66**, 035110 (2002).
- ¹⁷ N. L. Wang, P. Zheng, J. L. Luo, Z. J. Chen, S. L. Yan, L. Fang, Y. C. Ma, *Phys. Rev. B* **68**, 054516 (2003).
- ¹⁸ F. Marsiglio, J. P. Carbotte, and E. Schachinger, *Phys. Rev. B* **65**, 014515 (2001).
- ¹⁹ W. Zimmermann, E. H. Brandt, M. Bauer, E. Seider, and L. Genzel, *Physica C* **183**, 99 (1991).
- ²⁰ H. Matsui, K. Terashima, T. Sato, T. Takahashi, S.-C. Wang, H.-B. Yang, H. Ding, T. Uefuji, and K. Yamada, *Phys. Rev. Lett.* **94**, 047005 (2005).
- ²¹ T. Tohyama and S. Maekawa, *Phys. Rev. B* **64**, 212505 (2001).
- ²² Y. Dagan, M. M. Qazilbash, C. P. Hill, V. N. Kulkarni, and R. L. Greene, *Phys. Rev. Lett.* **92**, 167001 (2004).
- ²³ D. van der Marel, H. J. A. Molegraaf, J. Zaanen, Z. Nussinov, F. Carbone, A. Damascelli, H. Eisaki, M. Greven, P. H. Kes, and M. Li, *Nature (London)* **425**, 271 (2003).